



Modelling carbon dioxide adsorption behaviour on montmorillonite at supercritical temperatures

Gopika Raveendran¹ · Kumbamutlang War¹ · D. N. Arnepalli¹ · V. B. Maji¹

Received: 17 January 2024 / Revised: 14 July 2024 / Accepted: 15 July 2024

© The Author(s), under exclusive licence to Springer Science+Business Media, LLC, part of Springer Nature 2024

Abstract

Expandable clay minerals play a pivotal role in the geological sequestration of greenhouse gases due to their contribution to storage capacity and caprock integrity. The charge-balancing cations in the interlayer space are known to influence carbon dioxide adsorption. The present study investigated the general adsorption behaviour and characteristics of montmorillonite towards CO₂ adsorption at temperatures above critical point, typical to geological sequestration. Modelling on the excess isotherm and absolute isotherm was used to compare the variation of the adsorption behaviour of sodium, potassium and calcium montmorillonite. Excess isotherm modelling using the monolayer Ono-Kondo (O-K) model successfully captured the experimental adsorption. The lateral interaction of the adsorbed molecules on the montmorillonite surface, a variable with the type of cation, remarkably affected the strength of adsorption. The derived adsorbed phase density data confirmed the onset of swelling in montmorillonite at pressures below the critical point. Additionally, the study comprehended the influence of approximations used to derive the absolute isotherm from the experimental isotherm and investigated the validity of common theoretical models to represent adsorption. The study recommended the application of Dubinin-Astakhov (D-A) isotherm with reciprocal van der Waals density approximation or liquid density approximation to model the adsorption of CO₂ on montmorillonite.

Keywords Carbon dioxide adsorption · Isotherm modelling · Adsorption thermodynamics · Homoionized montmorillonite · Geological sequestration

Abbreviations

C	Adsorption capacity
E	Characteristic adsorption energy
k	Boltzmann constant
M	Molar mass of the gas
N	Degree of structural heterogeneity
P	Gas pressure
P ₀	Atmospheric pressure

P _c	Critical pressure
P _L	Langmuir pressure constant
P _s	Saturation pressure
q ₀	Limiting adsorption by micropore filling
q _a	Absolute adsorption
q _e	Excess adsorption
R	Universal gas constant
T	Adsorption temperature
T _b	Boiling point at atmospheric condition
T _c	Critical temperature
V _L	Langmuir volume constant
z ₀	Volume coordination number
z ₂	Monolayer coordination number
ε _{ff}	Fluid-fluid interaction potential
ε _{fs}	Fluid-solid interaction potential
ρ _a	Adsorbed phase density
ρ _b	Bulk phase density
ρ _{mc}	Adsorbed phase density at maximum capacity

✉ D. N. Arnepalli
arnepalli@iitm.ac.in
Gopika Raveendran
gopika.raveendran02@gmail.com
Kumbamutlang War
bamutknit08@gmail.com
V. B. Maji
vbmaji@iitm.ac.in

¹ Department of Civil Engineering, IIT Madras, Chennai 600036, India

1 Introduction

Being the primary contributor to global warming, carbon dioxide removal (CDR) has been identified as a measure of utmost significance to mitigate the impacts of global warming and related climate change. The Intergovernmental Panel for Climate Change (IPCC) emphasizes the importance of CDR in achieving net negative emissions by incorporating other mitigation measures [25]. As such, storage of CO₂ in geological formations (geosequestration) can trap CO₂ for a geologically significant time scale. Sedimentary formations with adequate porosity and permeability can be potential storage sites for carbon dioxide geological sequestration. For example, deep saline aquifers, active or depleted oil and gas reservoirs, coal seams, salt caverns, etc., are some of the formations with adequate capacity to store CO₂ [24]. Many researchers have investigated the feasibility, storage capacity and efficiency of such formations [5, 9, 41]. The significant risks associated with the storage of CO₂ underground arising from leakage have been studied. As such, the sealing efficiency of the reservoir caprocks was also investigated [6, 14, 38, 51].

Even though among all the trapping mechanisms (capillary, solubility, sorptive and structural trapping), sorptive trapping via adsorption contributes the least towards the storage [7], it is still considered significant in geosequestration as it is the initial stage of other long-term chemical interactions like precipitation and dissolution of the formation material [8]. Carbon dioxide adsorption on clay minerals present in the reservoir and caprock of the geological formation has emerged as a topic of interest owing to its contribution to both the storage and caprock integrity. The adsorption of CO₂ on the reservoir formations and caprocks predominantly occurs on the inorganic clay minerals and the organic content. Busch et al. [5] postulated that the inorganic content of the caprocks is of primary influence on its adsorption capacity. The experiments on the Muderong shale with a total organic content (TOC) of less than 0.5% demonstrated that the high adsorption capacity was attributed entirely to the reactive nature of its inorganic content.

Clay minerals are excellent adsorbents for CO₂ and have proven effective in capturing and storing CO₂ in them [34, 44]. The high degree of heterogeneity in the physical and chemical properties of clay makes the adsorption mechanism complex. Changes in mineralogy also add to the difference in adsorption in the clay minerals. Clay minerals falling under the class of smectites are of particular importance since these minerals can exhibit volumetric expansion upon CO₂ adsorption [13, 21, 35, 52]. Yin et al. [53] observed changes in pore structure in the shale caprocks after exposure to CO₂, attributed to the adsorptive swelling of clay minerals. This adsorption-induced swelling seals off

the fractures in the caprocks, enabling storage longevity [7]. Many researchers have reported the effect of the hydration state of smectite and the interlayer cation present in it on the magnitude of swelling. Giesting et al. [15] studied the adsorption-induced swelling of Na-montmorillonite and the dependence of the initial interlayer d-spacing of the mineral on CO₂ adsorption. Under high pressure and temperature, adsorption results showed that the intercalation of CO₂ was complete when the pressure reached around 5 MPa, beyond which the increase in pressure did not cause a change in interlayer space. Also, the study emphasized the requirement of a mixed layer of water molecules in the interlayer, i.e., 0 W or the complete absence of the water molecule and 1 W or the presence of a single plane of the water molecule, for maximum CO₂ intercalation. Rother et al. [45] reported a swelling of 4% with a sub-monolayer hydration state, i.e., an initial hydration state less than 1 W, for Na-montmorillonite, which was lower than the swelling reported by Giesting et al. [15], the difference being attributed to the higher number of 0 W states in the latter. Further, many researchers emphasized the necessity of the presence of sub-monolayer H₂O for CO₂ intercalation on smectites [22, 30, 46, 47]. Interlayer cations having high hydration energy and small ionic radii (e.g. Na⁺ and Ca²⁺) need H₂O molecules to prop open the interlayers for CO₂ to enter the interlayer space [18, 20]. On the other hand, for minerals with interlayer cations of low hydration energy and large ionic radii (e.g. K⁺ and Cs⁺), CO₂ can easily enter the interlayer space in the complete absence of H₂O, the reason being that the energy barrier for CO₂ to enter the interlayer space decreases as the size of the cation increases [4, 29].

The focus of much of the work conducted in the CO₂ adsorption of clay minerals was on the swelling mechanism that occurs in the interlayer space. However, for understanding the effect of interlayer cation in smectites on the CO₂ adsorption behaviour, adsorption occurring on all exposed surfaces of the mineral, including the edges, has not been investigated systematically. This implies the need for adsorption isotherm modelling to apprehend the adsorption behaviour of clay minerals towards CO₂ adsorption. Numerous CO₂ adsorption isotherm modelling studies have been conducted on shale caprocks in the recent past to get a comprehensive understanding of the CO₂ adsorption behaviour on shale caprocks. Experimental CO₂ studies on shale samples by Mahmoud et al. [31] concluded that Freundlich and Brunauer-Emmett-Teller (BET) isotherms describe the adsorption in shale better than Langmuir isotherm. On the contrary, Zhou et al. [54] concluded that the Dubinin-Astakhov (D-A) model for sub-critical CO₂ and the Ono-Kondo (O-K) model for ScCO₂ showed the best fit for the experimental data on shale samples. Further, Merey and Sinayuc [33] demonstrated that the monolayer O-K

model could be a better alternative than Langmuir for high-pressure CO₂ adsorption on shale samples. The difference in the isotherm modelling suggests that for an entirely different sample taken from a different location, these results may not be sufficient to predict the adsorption mechanism in shale in general. Besides, it implies that CO₂ adsorption modelling on shale is predominantly influenced by the structural, compositional, and energetic heterogeneity in the shale, as well as the difference in depositional setting and features. Therefore, the CO₂ adsorption isotherm modelling on the individual composition of caprocks can shed light on understanding the underlying mechanism.

Although many authors [33, 40, 50] have recognized Local Density Functional Theory (LFDT) to model adsorption, studies on the CO₂ adsorption modelling on clay minerals at moderate temperature and pressure conditions are a few. For instance, Hwang et al. [23] modelled supercritical CO₂ adsorption on montmorillonite source clay using Local Density Functional Theory (LFDT) and emphasized the potential of LFDT to predict the adsorption behaviour as compared to empirical models like Langmuir. Moreover, the inherent physical heterogeneity in smectites due to the interlayer cation present results in differences in adsorption [43]. The present work focuses on the CO₂ adsorption isotherm modelling on sodium, potassium and calcium montmorillonite. For this purpose, CO₂ adsorption experiments were conducted at a temperature range significant to the geological sequestration and isotherm modelling was done to investigate the factors affecting the development of the adsorbed phase on the surface of each of the homoionized samples. Since the influence of the change in surface characteristics with change in cation is expected to be the highest in the first layer of adsorption, adsorption up to a pressure of 5 MPa (pressure below phase transition) was chosen to ensure monolayer adsorption. The adsorption temperature was selected assuming a storage reservoir of a minimum depth of 700 m and a geothermal gradient of 0.02 °C·m⁻¹-0.03 °C·m⁻¹. Accordingly, the adsorption temperatures were chosen to be 35°C, 45°C and 55°C. Also, thermodynamic interpretation of the adsorption isotherm was performed to contemplate the modelling results, i.e., the strength and capacity of the montmorillonite to hold CO₂.

2 Experimentation

2.1 Characterization and sample preparation

Commercially available sodium montmorillonite was used to prepare the homoionized montmorillonite samples used in the study. The specific gravity of the pristine mineral was estimated to be 2.78 according to ASTM

D5550 [3]. The XRF analysis on the pristine mineral was done to estimate the chemical composition of montmorillonite. As per the analysis, selected montmorillonite composition includes 57.5% SiO₂, 15.3% Al₂O₃, 13.7% Fe₂O₃, and 13% other oxides in trace quantities. For the preparation of homoionized samples, the as-received montmorillonite was first washed with deionized water (10 g of soil in 100 ml deionized water) and mixed in a mechanical shaker to extract all the soluble ions. The soil solution, after mixing, was centrifuged at 1600 rpm for 30 min to separate the soil from the solution. This process was repeated until the electrical conductivity of the supernatant solution reached that of deionized water. After the complete removal of dissoluble cations, homogenization was carried out by treating oven-dried samples with the aqueous solutions of sodium chloride, potassium chloride, and calcium chloride to obtain sodium exchanged- (MT-Na), potassium exchanged- (MT-K), and calcium exchanged-montmorillonite (MT-Ca). To ensure a complete exchange of cations, the samples were repeatedly equilibrated with the respective aqueous chloride solutions [42]. After each treatment, the soil was separated from the solution, and the concentration of the respective cation in the supernatant was analyzed using an Atomic Absorption Spectrometer (Thermoscientific, USA). The process was repeated until the cation concentration retained in the solution became constant. Further, the chloride content was removed from the homoionized montmorillonite by washing it with deionized water. All the samples thus prepared were oven dried at 110 °C for 24 h and then vacuum stored in a desiccator before performing adsorption experiments.

2.2 Adsorption experiments

The CO₂ adsorption experiments were performed on dry powdered samples using a high-pressure sorption analyzer (iSorb, Quntachrome, USA) at 35 °C, 45 °C, and 55 °C. The initial void volume of the samples was measured using helium gas before allowing the CO₂ to interact with the samples. High-purity carbon dioxide (99.999%) and helium (99.99%) were used in the experiments. The experimental setup includes gas inlets, a section of a known volume called the manifold, and a thermostated zone for connecting the sample cell. The manifold temperature was maintained at 45 °C during the void volume calibration for all the experiments to ensure uniformity in experimentation.

All the samples were degassed initially to remove all adsorbed moisture and gases from the samples. The degassing temperature was chosen based on the thermal decomposition signature of the homoionized samples (at 10 °C·m⁻¹ in nitrogen atmosphere), obtained based

on thermogravimetric analysis (TGA) using ‘SDT 650’ (TA instruments, USA). The samples were subjected to an absolute vacuum while increasing their temperature to the desired degassing temperature. CO₂ was allowed to expand into the manifold and reach pressure equilibrium before introducing it into the sample cell. The gas pressure in the cell was increased in the required pressure increments, keeping the sample cell temperature at the required temperature (isothermal). After each pressure increment (up to a maximum pressure of 5 MPa), the sample cell pressure was allowed to equilibrate, and the number of moles adsorbed per gram of adsorbent was measured based on the corresponding drop in pressure at each increment. To account for the adsorption of CO₂ on the sample cell walls, blank-run experiments were performed using an empty cell at each of the analysis temperatures.

2.3 Specific surface area

The BET-specific surface area (SSA) of all samples after homogenization was determined using ‘Autosorb iQ’ (Quantachrome, USA). Nitrogen adsorption experiments at 77 K were conducted on the clay samples over a pressure range (P/P_0) of 0.05 to 0.35 where P_0 is the measured atmospheric pressure. All the samples were degassed to evacuate the pre-occupied gases and moisture within the sample before performing the nitrogen adsorption.

3 Isotherm modelling

The adsorption measurements from the experimentation underestimate the actual amount of gas adsorbed [37]. This is because of the practical difficulties in the experimentation, which arise due to the existence of entrapped gas molecules in the adsorbed volume. The measurable quantity, called the excess adsorption (q_e) corresponds to the number of moles obtained directly from the drop in pressure in the system upon the adsorption process. With progressing adsorption, the void volume available gets reduced due to the formation of the adsorbed phase, which is not measurable during the adsorption. This further reduces the excess adsorption from the actual adsorption. If ρ_a is the density of the adsorbed phase and ρ_b is the gas density in the bulk phase, the absolute adsorption (q_a) is estimated as

$$q_a = q_e \left(\frac{\rho_a}{\rho_a - \rho_b} \right) \quad (1)$$

The difference between the excess and absolute may be too small at low pressure, but it becomes significant as the

pressure increases. For adsorption isotherm modelling, the selection of data (excess or absolute), therefore, affects the interpretation of results.

3.1 Excess isotherm modelling

Excess isotherm was modelled using O-K model [39]. This model incorporates the effects of the interaction between the adsorbate and the adsorbent surface (ϵ_{fs}), the interaction among the adsorbates (ϵ_{ff}), and the adsorbent pore geometry on adsorption. The increase in the adsorbed phase density with adsorption is considered in the model, making it suitable for extracting the information on absolute isotherm from the excess isotherm. The O-K model describes the adsorbent surface as a discrete distribution of pore spaces called a lattice that can hold gas molecules. The model relates the density on any specific lattice site to the density on the adjacent sites and the density in the bulk phase. Using this theory, the thermodynamic equilibrium for monolayer adsorption of a gas on an adsorbent surface is expressed as follows [2]

$$\ln \left[\frac{x_a(1-x_b)}{x_b(1-x_a)} \right] + \frac{(z_2x_a - (z_0 - z_1)x_b)\epsilon_{ff}}{kT} + \frac{\epsilon_{fs}}{kT} = 0 \quad (2)$$

In the above expression, k is the Boltzmann constant, T is the absolute temperature, x_a is the fraction of sites occupied by adsorbed phase molecules, given by $x_a = \rho_a/\rho_{mc}$, and x_b is that occupied by bulk phase molecules, given by $x_b = \rho_b/\rho_{mc}$. ρ_a , ρ_b and ρ_{mc} are the adsorbed phase density, bulk phase density, and adsorbed phase density at maximum capacity, respectively. The density of the CO₂ in the bulk phase was calculated using the Helmholtz equation of state [49]. z_0 represents the volume coordination number, z_2 represents the monolayer coordination number, and $z_1 = (z_0 - z_2)/2$. For the hexagonal closest packing of lattice cells, z_0 and z_2 are 12 and 6, respectively.

Gibbs excess adsorption assuming slit pore is expressed as [50]

$$\Gamma = 2C(x_a - x_b) \quad (3)$$

To reduce the complexity of the regression involved in solving for four unknown parameters (ϵ_{ff} , ϵ_{fs} , ρ_a , and ρ_{mc}), the model was reduced to a two-parameter model [50]. The adsorbate-adsorbate interaction energy (ϵ_{ff}) and the adsorbed phase density at maximum capacity (ρ_{mc}) were estimated theoretically, but the adsorbate-adsorbent energy parameter (ϵ_{fs}) and the parameter C were regressed in the model using the experimental excess adsorption data.

Assuming the real and lattice fluids’ critical temperature (T_c) is the same, the pairwise interaction between the

adsorbate molecules can be estimated [40]. The adsorbate-adsorbate interaction energy (ϵ_{ff}) is accounted for using the following relationship.

$$\frac{|\epsilon_{ff}|}{k} = \frac{4T_c}{z_0} \quad (4)$$

The adsorbed density at maximum capacity is taken as proportional to the reciprocal of van der Waals co-volume [12]. That is,

$$\rho_{mc} = 8P_cM/RT_c \quad (5)$$

where M is the molar mass of the CO_2 . The calculated input parameters for CO_2 as adsorbate are $|\epsilon_{ff}/k| = 101.4 \text{ K}$ and $\rho_{mc} = 23.34 \text{ mol}\cdot\text{L}^{-1}$.

The model parameters are optimized by taking the minimum χ^2 error given by

$$\chi^2 = \sum \left[\frac{(q_{model,i} - q_{e,i})^2}{q_{e,i}} \right] \quad (6)$$

where $q_{e,i}$ and $q_{model,i}$ are the excess adsorption obtained from the experiment and the that fitted using the O-K model corresponding to each pressure increment, respectively.

Equations 2 and 3 were later used to find the adsorbed phase density at each of the pressure increments, which were further used to obtain the absolute isotherm. The absolute isotherms thus obtained were compared with approximate isotherms calculated by assuming a constant density for the adsorbed phase. Table 1 lists the physical properties of CO_2 used throughout the study.

3.2 Absolute isotherm modelling

Various theoretical isotherms were used by researchers to describe the adsorption of CO_2 [11, 17, 23, 33, 54]. The theoretical basis on which these isotherm equations were formulated aids in describing the mechanism of adsorption. In this study, two theoretical models representing homogeneous adsorption and heterogeneous adsorption were selected, thereby estimating the effect of the surface energy heterogeneity towards CO_2 adsorption on montmorillonite. Langmuir (homogeneous adsorption) and

D-A (heterogeneous adsorption) equations were used to model the absolute isotherms.

The Langmuir isotherm model is the most common and simplest isotherm used widely to represent gas adsorption. The model assumes monolayer coverage and energy homogeneity of the adsorbent surface. It does not take into consideration the interaction between the adsorbed molecules. The Langmuir isotherm equation is as follows [27].

$$q_a = \frac{V_L P}{P_L + P} \quad (7)$$

where V_L and P_L are the Langmuir constants and P is the equilibrium pressure. V_L is related to the monolayer capacity, and P_L is the pressure required for the adsorption to reach half the monolayer capacity.

D-A isotherm model is based on the theory of micropore filling. According to this theory, the adsorption occurs by pore-filling mechanism rather than monolayer coverage on discrete pores. The D-A model equation is as follows [10].

$$q_a = q_0 \exp \left[-D \left(\ln \frac{P_s}{P} \right)^n \right] \quad (8)$$

$$D = \left(\frac{RT}{E} \right)^n \quad (9)$$

where q_0 is the limiting amount of adsorption by micropore filling, D is the model constant for a particular adsorbent-adsorbate system, E is the characteristic energy of adsorption, P_s is the saturation pressure, and n is the degree of structural heterogeneity of the adsorbent. Saturation pressure in the present study becomes meaningless as the temperature range is above the critical value. Li and Gu [28] suggested using quasi-saturated vapour pressure for the D-A equation in supercritical adsorption. They proposed the following equation for a reference temperature (ratio of adsorption temperature to critical temperature of the adsorbate) in the range 1 to 1.8.

$$P_s = P_c \exp \left[h \left(1 - \frac{T_c}{T} \right) \right] \quad (10)$$

$$h = \frac{T_b}{T_c \left[\frac{\ln P_c}{1 - T_b/T_c} \right]} \quad (11)$$

where P_c , T_c , and T_b are the critical pressure, the critical temperature, and the boiling point of CO_2 at atmospheric pressure, respectively (Table 1).

Table 1 Physical properties of CO_2

Property	Value
Critical pressure, P_c (MPa)	7.377
Critical temperature, T_c (K)	304.130
Boiling point at atmospheric condition, T_b	194.670
Critical density ($\text{mol}\cdot\text{L}^{-1}$)	10.625
Liquid density ($\text{mol}\cdot\text{L}^{-1}$)	26.777

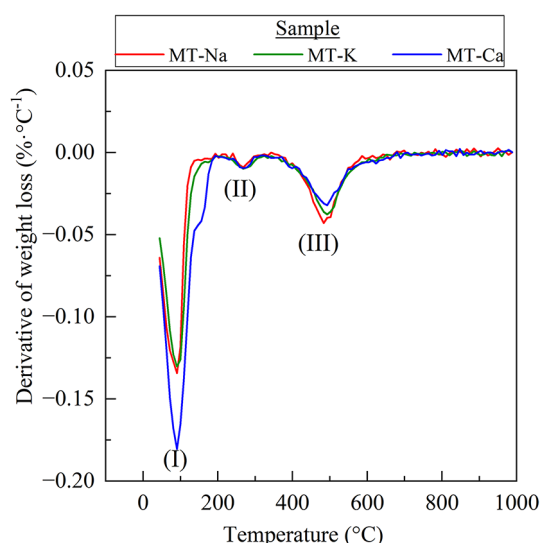


Fig. 1 Thermogravimetric analysis of the homoionized montmorillonite samples

Table 2 Specific surface area and ionic potential of the homoionized montmorillonite

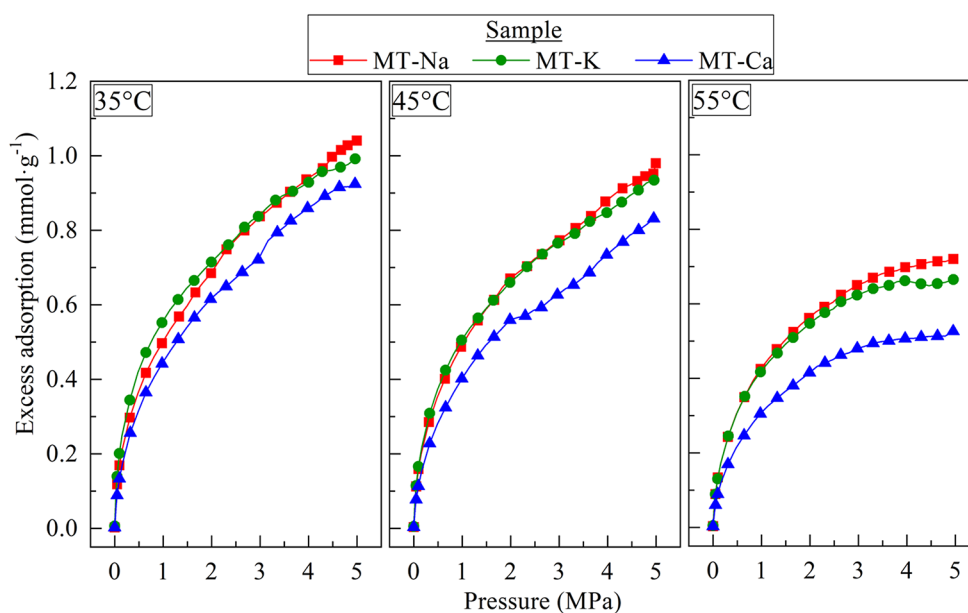
Sample	BET surface area ($\text{m}^2 \cdot \text{g}^{-1}$)	Hydrated ionic radius of the charge-balancing cation* (\AA)	Ionic potential of the charge balancing cation
MT-Na	86.093	2.32	0.362
MT-K	60.444	2.76	0.431
MT-Ca	47.857	4.10	0.488

* Adapted from Shannon [48]

4 Results and discussion

4.1 BET surface area and excess isotherm

Fig. 2 Excess isotherm for all the samples tested at different temperatures



The degassing temperature was chosen to remove free and adsorbed interlayer water completely; however, the charge-balancing cations remain hydrated. From the thermogravimetric analysis (TGA) plot (Fig. 1), three peaks were identified. Peak I (100–200 °C) corresponds to the removal of free and loosely bound interlayer water, peak II (200–300 °C) corresponds to the removal of strongly bound water from the first coordination sphere of the charge balancing cation, and peak III (400–600 °C) corresponds to the dehydroxylation of the clay mineral [19]. Hence, the degassing temperature was fixed at 180 °C, slightly less than 200 °C for all the analyses.

The estimated values of BET surface area of the montmorillonite samples with different charge balancing cations and the ionic properties of the respective cations are presented in Table 2. The ionic potential of the cation is estimated as the ratio of the valency of the cation to the ionic radius. The experimental excess isotherms obtained for montmorillonite samples with different charge balancing cations show a decreasing trend with temperature, which is typical for any physisorption system (Fig. 2).

4.2 Excess adsorption modelling

The excess isotherm modelling was done by solving the O-K model equations (the detailed estimates obtained from O-K modelling for all samples are provided in supplementary data).

The parameter C is related to the capacity of the clay surface to adsorb CO_2 and ϵ_{fs} signifies energy associated with the CO_2 -clay surface interaction. A higher value of ϵ_{fs} would indicate a higher amount of energy would be required to desorb the molecule from the adsorbed state. These

Fig. 3 Variation of **a)** adsorption capacity, i.e., parameter C and **b)** fluid-solid energy parameter with temperature

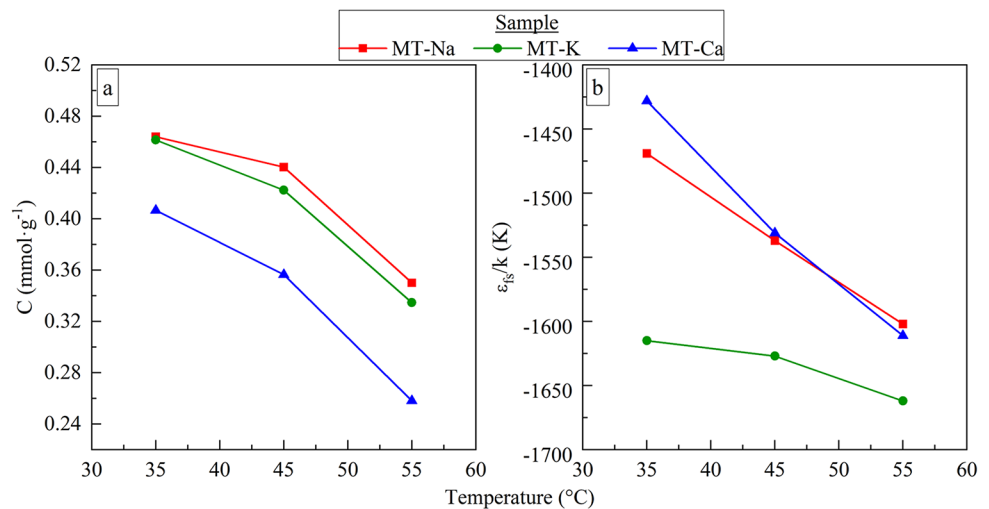
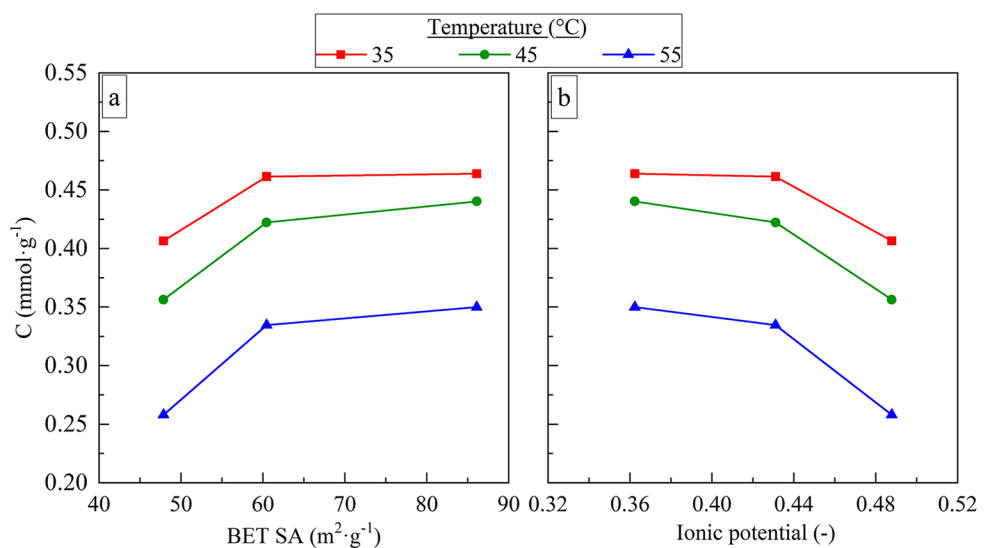


Fig. 4 Variation of parameter C with **a)** BET surface area and **b)** ionic potential



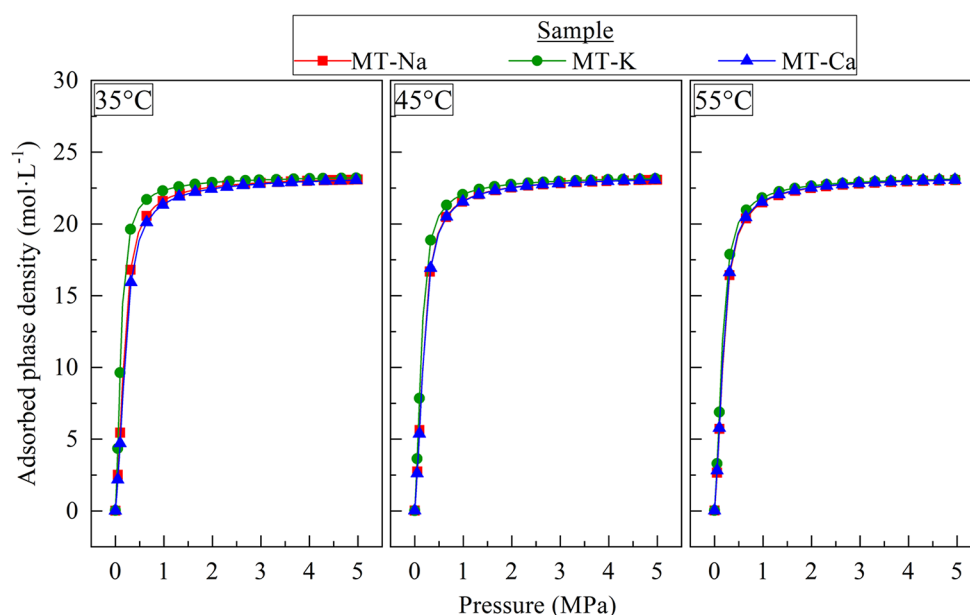
fitted parameters in the O-K model (C and ϵ_{fs}) are found to decrease with increasing temperature (Fig. 3). However, both these parameters increase with the increase in the absolute adsorption at the maximum pressure of 5 MPa obtained from the model. Further, the fitted parameters are compared based on the BET surface area of the samples and the ionic potential of the charge-balancing cations.

The variation of the parameter C with the measured specific surface area of the montmorillonite samples (Fig. 4) confirms that the increase in absolute adsorption at the maximum pressure of 5 MPa with the parameter C is due to its dependence on the specific surface area. Increasing specific surface area ensures more availability of the active site for the adsorption of CO_2 on the clay mineral surface. This agrees with the study by Mendel et al. [32]. Also, with the increase in ionic potential (ratio of valency to the cation by the respective hydrated ionic radius), the parameter C is reduced, hence, the absolute adsorption.

The more negative value of ϵ_{fs}/k suggests stronger adsorption with an increase in temperature. Still, it does not influence the maximum adsorption (Fig. 3). Although the value of ϵ_{fs}/k is varying with temperature for all the samples, the normalization concerning temperature (ϵ_{fs}/kT) results in negligible difference within the sample (Refer to supplementary data).

The adsorbed phase density followed the same trend with an increase in pressure for all the homoionized samples irrespective of the adsorption temperatures (Fig. 5). As adsorption progressed, the adsorbed phase's initial development was rapid, marked by a steep rise in adsorbed phase density. Thereafter, the change in adsorbed phase density reduces, and the adsorbed phase density reaches a constant of around 2.5 MPa for all the samples, indicating an expansion in the adsorbed phase volume in this stage, initiating the swelling process with further adsorption. At 35 °C, there is a distinct difference in the adsorbed phase densities of the montmorillonite samples, which diminishes

Fig. 5 Comparison of change in adsorbed phase densities with equilibrium pressure



as the temperature increases, indicating that the effect of charge balancing cation towards the development of the adsorbed phase is significant at 35 °C. However, the maximum adsorbed phase density remains unchanged with the change in adsorption temperature. Hence, the increase in absolute adsorption at each adsorption temperature suggests a temperature-independent expansion of the adsorbed phase volume over the montmorillonite surface during adsorption.

4.3 Comparison of the model derived absolute isotherm with approximate estimations

In contrast to the obtained adsorbed phase density variation with pressure increment, a general empirical approach to estimating the absolute adsorption assumes a constant density of the adsorbed phase. The commonly used constant density approximations take the density of the adsorbed phase to be either (a) reciprocal van der Waals co-volume, (b) critical density, or (c) liquid density. The consideration of van der Waals co-volume assumes the molecules in adsorbed phase to have the van der Waals excluded molar volume. Also, as the adsorbed phase hosts the molecules in the limited pore spaces, the assumption of critical density or liquid density guarantees a higher density than the gas phase.

The absolute isotherm obtained from the O-K model and the absolute isotherm estimated using the explained constant density approximations for 35 °C are compared (Fig. 6). Refer supplementary data for the coefficient of determination (R^2) values obtained for the fit for each of the approximations. Though the adsorbed phase density is found to increase with pressure, the consideration of a constant adsorbed phase density equal to reciprocal van

der Waals co-volume ($23.34 \text{ mol}\cdot\text{L}^{-1}$ for CO_2) and liquid density ($26.77 \text{ mol}\cdot\text{L}^{-1}$) adjusts the calculation for the absolute adsorption matching the absolute adsorption obtained from the O-K model. This is because the maximum adsorbed phase density attained in each sample remains around $23 \text{ mol}\cdot\text{L}^{-1}$ up to a pressure of 5 MPa for all the adsorption temperatures considered. Besides, it is observed that the critical density approximation overestimates the absolute adsorption as pressure increases. Similar results were obtained for isotherms at 45 °C and 55 °C, suggesting that both reciprocal van der Waals constant density approximation and liquid density approximation can be relied on to estimate the absolute quantities for the modelling and thermodynamic analysis of adsorption up to 5 MPa.

Despite the simplicity of calculation involved in the estimation of absolute adsorption using the above empirical methods, it is to be noted that these methods lack the theoretical background. These methods assign the adsorbed phase density a value that is independent of the characteristics of the adsorbent. The approximations are specific to an adsorbate molecule irrespective of the adsorption temperature or pressure, which makes it conceptually non-realistic.

4.4 Adsorption thermodynamics

Estimating the isosteric heat of adsorption (Q) aids in identifying the nature and strength of adsorption. It can be determined using the Clausius-Clapeyron equation as follows.

$$Q = -R \left[\frac{d(\ln P)}{d(1/T)} \right]_{q_a} \quad (12)$$

Fig. 6 Comparison of absolute adsorption estimates for 35 °C from **a)** reciprocal van der Waals approximation, **b)** liquid density approximation and, **c)** critical density approximation with O-K model estimate (open symbols indicate the absolute adsorption estimates from O-K model; dash line indicates the absolute adsorption estimates from the theoretical approximations)

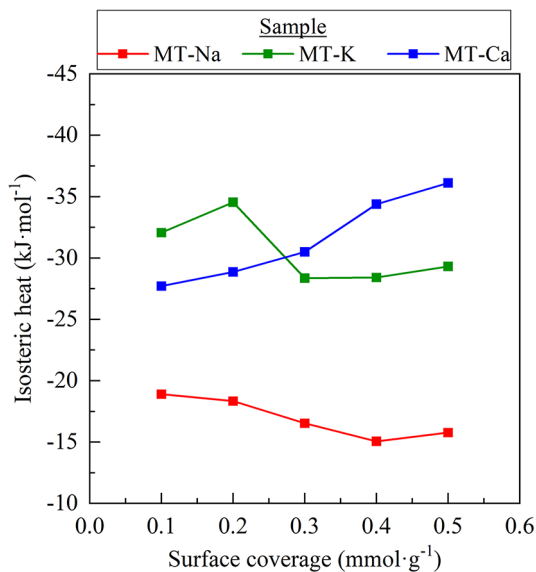
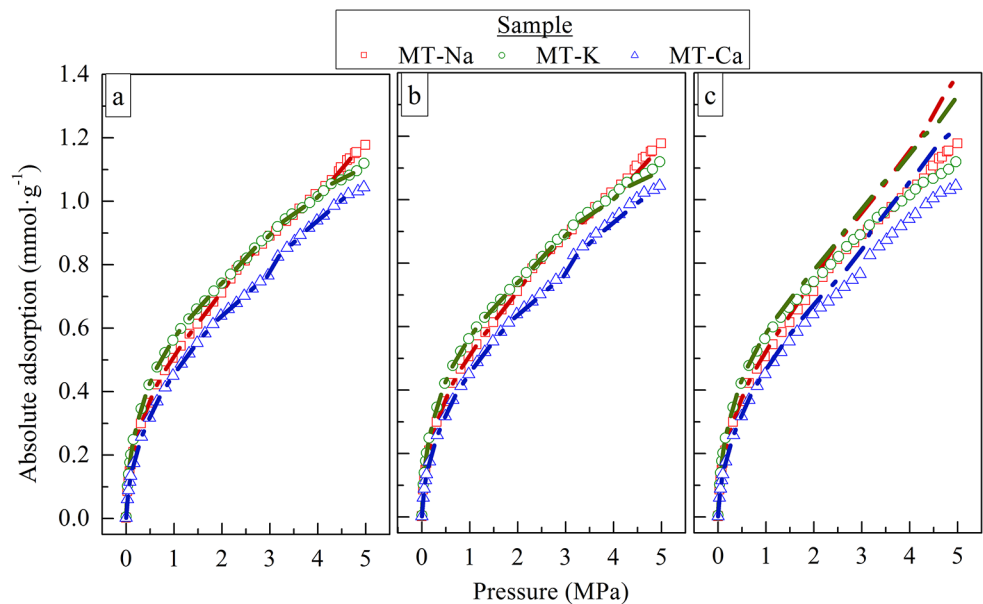


Fig. 7 Isothermic heat of adsorption distribution

The slope of the plot between the $\ln P$ and $1/T$ for a constant absolute surface coverage gives the isothermic heat of adsorption. The distribution of isothermic heat of adsorption for the samples indicates the mechanism of adsorption (Fig. 7). The absolute adsorption data obtained from the O-K model is used to indicate the surface coverage. The low isothermic heat (less than $40 \text{ kJ}\cdot\text{mol}^{-1}$) for all the samples confirms that the CO_2 adsorption in such cases is by physisorption characterized by electrostatic and van der Waals interaction [36]. This is in agreement with the study by Jedli et al. [26] which reported CO_2 physisorption on clay-rich caprocks. The variation in isothermic heat with surface coverage is due to the surface energy heterogeneity of the montmorillonite samples. Only the adsorption sites with the highest energy

can hold the CO_2 molecules on the surface at low-pressure conditions. Any reduction in isothermic heat with surface coverage results from the adsorption on the low-energy sites. At the same time, the increase in isothermic heat with surface coverage is due to the lateral interaction between the adsorbed molecules [1].

At low surface coverage, MT-K exhibits the highest isothermic heat since it had the highest CO_2 -clay mineral surface interaction energy (as seen from the O-K model), favouring the adsorption in the highest energy sites on its surface. As the adsorption progresses with the increase in bulk CO_2 pressure, the lower energy sites also get filled, lowering the isothermic heat, and the interaction between the adsorbed molecules strengthens. This stage is marked by a slight increase in isothermic heat, which is visible in MT-K and MT-Na. However, the isothermic heat increases with adsorption for MT-Ca due to the low CO_2 -clay mineral surface interaction energy for MT-Ca (obtained from the O-K model). For MT-K, besides CO_2 -clay mineral surface interaction, there is a significant contribution from the lateral interaction between the adsorbed CO_2 molecules towards adsorption. Whereas, in MT-Na, the contribution from CO_2 -clay mineral surface interaction is much higher than the lateral interaction between the adsorbed CO_2 molecules. However, for MT-Ca, the effect of lateral interaction between the adsorbed CO_2 is predominant in MT-Ca. Hence, it can be confirmed from the isothermic heat distribution and the O-K model that the strength of adsorption follows the order $\text{MT-K} > \text{MT-Na} > \text{MT-Ca}$.

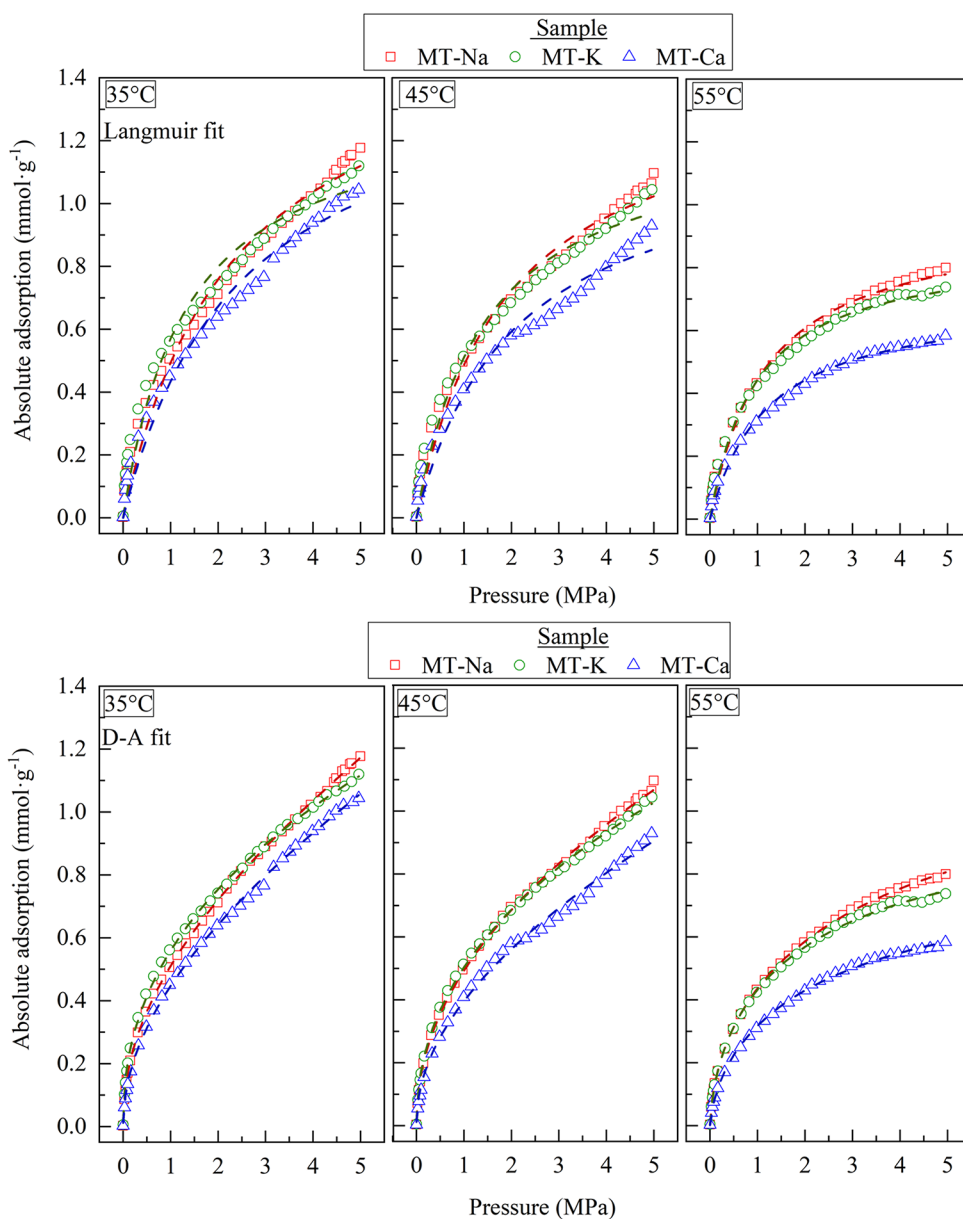
4.5 Absolute isotherm modelling

Langmuir and D-A isotherms were also fitted to the estimated absolute data obtained for each sample at all the test temperatures (Fig. 8). The results of the isotherm modelling reveal that both models can well correlate the adsorption of CO₂ on montmorillonite.

The root means square errors for the model fitting were also compared to obtain the best-fit model for representing CO₂ adsorption on montmorillonite. The root mean square error is calculated as

$$RMSE = \sqrt{\frac{\sum_{i=1}^N (q_{a,i} - q_{fit,i})^2}{N}} \quad (13)$$

Fig. 8 Absolute isotherm modelling (open symbols indicate absolute adsorption estimates from O-K model; dash line indicates theoretical model fit)



where $q_{a,i}$ and $q_{fit,i}$ are the calculated absolute adsorption and the fit-predicted value at the same pressure, and N is the number of data points in the isotherm. Refer to the supplementary data for the calculated coefficient of determination (R^2) and RMSE values for each adsorption isotherm model.

As the RMSE values of D-A isotherm are much lower than Langmuir (Fig. 9), it can be concluded that the former can predict CO₂ adsorption on montmorillonite with high precision for all the temperature and pressure ranges considered in the study. However, for 55 °C, the error for Langmuir isotherm approaches that of the D-A isotherm for all the samples. This may be attributed to the low surface coverage at high temperature conditions. In other words, the assumption of a homogenous surface in the Langmuir model becomes invalid for adsorbents with surface imperfections

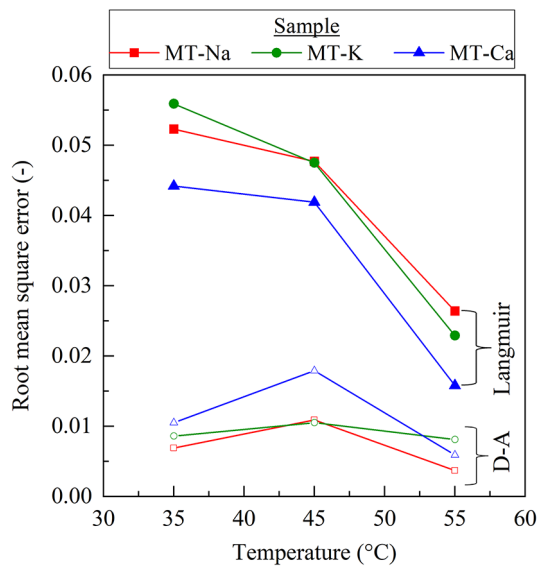


Fig. 9 Error analysis of fitted absolute isotherms (as observed from the calculated isosteric heat distribution)

and appreciable surface coverage. In contrast to this, the limitation in D-A model (non-existence of saturation pressure above critical temperature) when modified using the quasi-saturated vapor pressure enhances its ability to demonstrate CO₂ adsorption on montmorillonite at any temperature.

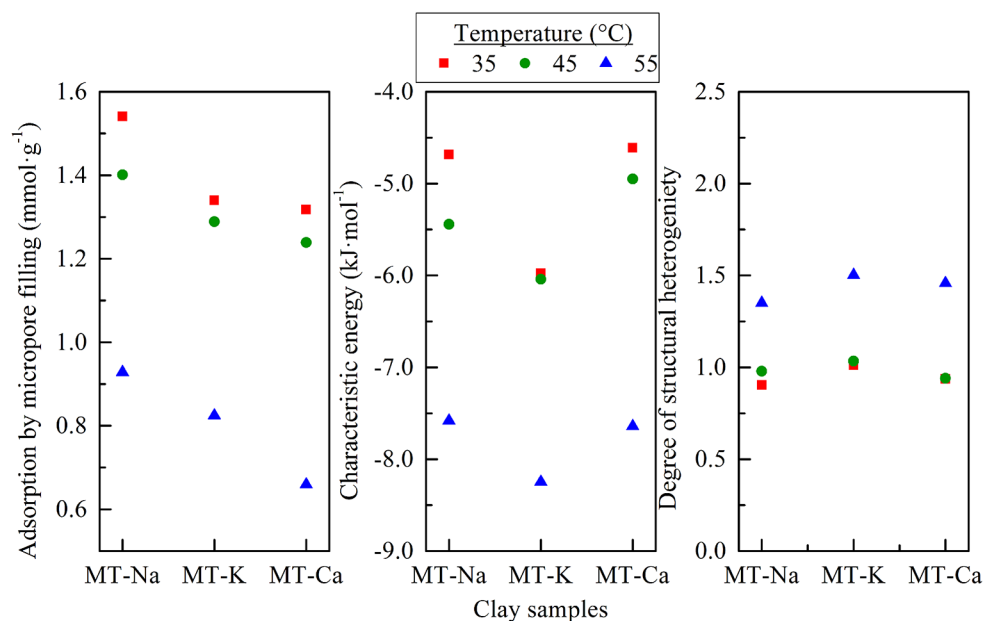
The model-derived parameters estimated are also compared (Table 3). It may be noted that there is a marked difference in the monolayer adsorption capacities estimated (V_L and q_0) depending on the choice of model. Hence, it is of utmost significance that the chosen model is appropriate to describe the adsorption behaviour with accuracy.

The D-A model-derived parameters were plotted to determine further the efficacy of using the D-A model to predict the adsorption behaviour of the montmorillonite at moderate temperature and pressure conditions (Fig. 10) and compared to the results of the excess O-K model. The variation of q_0 confirms a positive correlation with the specific surface area, as observed in O-K model. MT-Na, with the highest BET surface area had the maximum value of q_0 followed by MT-K and MT-Ca for all the adsorption

Table 3 Estimated parameters from absolute isotherm modelling

Sample	Temperature (°C)	Langmuir		D-A		
		V_L (mmol·g ⁻¹)	P_L (MPa)	D (-)	n (-)	q_0 (mmol·g ⁻¹)
MT-Na	35	1.640	2.321	0.580	0.903	1.541
	45	1.414	1.909	0.493	0.979	1.401
	55	0.962	1.166	0.251	1.350	0.928
MT-K	35	1.336	1.343	0.424	1.012	1.340
	45	1.253	1.455	0.425	1.034	1.289
	55	0.866	0.957	0.190	1.502	0.824
MT-Ca	35	1.496	2.444	0.576	0.936	1.318
	45	1.212	2.093	0.555	0.940	1.239
	55	0.709	1.207	0.223	1.458	0.659

Fig. 10 D-A model parameters for the montmorillonite samples with different charge balancing cations



temperatures considered emphasizing the significance of specific surface area on the adsorption capacity. The characteristic adsorption energy was calculated (Eq. 9) using the fitted parameter D obtained from the D-A model. The order of increase of the characteristic energy of adsorption follows the same order as the strength of interaction obtained from the O-K model. The effect of structural heterogeneity due to the effect of the pore size distribution is reflected in the value of the parameter n in the D-A model. For all the samples, the value of n lies within the range 0.9035–1.502, indicating a negligible difference in the structural heterogeneity with change in charge balancing cation towards CO₂ adsorption.

5 Summary and conclusions

The CO₂ adsorption behaviour of montmorillonite up to 5 MPa over a range of temperatures above the critical point was investigated using isotherm modelling. Excess isotherm modelling using the O-K model suggests the influence of the charge-balancing cation in montmorillonite on the capacity of adsorption and the strength of interaction between CO₂ and the clay mineral surface. The excess isotherm modelling and absolute isotherm modelling highlight the effect of specific surface area on the CO₂ adsorption capacity, confirming that a higher specific surface area yields higher CO₂ adsorption capacity. The progression of the adsorbed phase on the clay mineral surface was also captured. The conclusions drawn based on the findings of the study are as follows.

- The experimental excess adsorption of CO₂ on montmorillonite can be described by the O-K model in general, irrespective of the charge balancing cation.
- The contribution of CO₂-clay mineral surface interaction and the lateral interaction between the adsorbed CO₂ molecules influences the adsorption strength.
- The study indicates that a higher adsorption capacity does not guarantee a higher interaction strength since adsorption capacity measures the available adsorption sites, whereas the strength of interaction measures energy associated with adsorption. As such, sodium montmorillonite showed the maximum adsorption capacity due to its higher specific surface area, followed by potassium and calcium montmorillonites, whereas potassium montmorillonite showed the highest strength of adsorption owing to the least lateral interaction between the adsorbed molecules.
- The maximum adsorbed phase density reaches a horizontal asymptote with pressure above 2.5 MPa on the montmorillonite surface, irrespective of the cation type

and the adsorption temperature, indicative of the initiating swelling with subsequent adsorption.

- The accuracy of the prediction of D-A isotherm to describe CO₂ adsorption on montmorillonite was very high. However, the Langmuir model gives a close prediction to the D-A model as the temperature increases. Besides, the influence of exchangeable cation in CO₂ adsorption on montmorillonite in terms of specific surface area and the interaction energy obtained from the D-A model supports the findings from the excess isotherm modelling using the O-K model.
- Overall, the study recommends the use of the D-A model with reciprocal van der Waals density approximation or liquid density approximation for the absolute isotherm modelling to predict the CO₂ adsorption capacity and the adsorption thermodynamics of montmorillonite as long as the surface coverage remains monolayer.

The qualitative trends of CO₂ adsorption presented in this work may apply to montmorillonite with other charge-balancing cations. As such, it may be generalized that the sub-monolayer surface coverage in montmorillonite potentially generates swelling irrespective of the type of cation. In other words, CO₂ injection pressure as low as 2.5 MPa would be sufficient to cause the swelling phenomenon in the montmorillonite, which in turn assists the cap-rock integrity. The major conclusions from the study are believed to provide complementary insight into the CO₂ adsorption behaviour of montmorillonite.

Supplementary Information The online version contains supplementary material available at <https://doi.org/10.1007/s10450-024-00525-z>.

Acknowledgements The authors would like to acknowledge the Department of Science and Technology–Science and Engineering Research Board, India, for the financial support through EMR/2016/001152.

Author contributions Author 1: Gopika Raveendran: Data curation, Formal analysis, Investigation, Writing- Original draft. Author 2: Kumbamutlang War: Writing- Original draft. Author 3: D. N. Arnepalli: Conceptualization, Supervision, Validation, Writing-review & editing, Project administration, Funding acquisition. Author 4: V. B. Maji: Supervision, Validation, Writing-review & editing, Project administration, Funding acquisition.

Funding The research leading to these results received funding from the Department of Science and Technology–Science and Engineering Research Board, India, for the financial support through EMR/2016/001152.

Data availability No datasets were generated or analysed during the current study.

Declarations

Ethical approval Not applicable to the data associated with the manuscript.

Competing interests The authors declare no competing interests.

References

- Al-Muhtaseb, S.A., Ritter, J.A.: Roles of surface heterogeneity and lateral interactions on the isosteric heat of adsorption and adsorbed phase heat capacity. *J. Phys. Chem. B.* **103**(13), 2467–2479 (1999). <https://doi.org/10.1021/jp984110s>
- Aranovich, G.L., Donohue, M.D.: A new model for lattice systems. *J. Chem. Phys.* **105**(16), 7059–7063 (1996). <https://doi.org/10.1063/1.472507>
- ASTM D5550: Standard test Method for Specific Gravity of soil Solids by gas Pycnometer. ASTM International, West Conshohocken, Pennsylvania, USA (2006)
- Bowers, G.M., Schaef, T., Loring, H., Hoyt, J.S., Burton, D.W., Walter, S.D., E. D., and, Kirkpatrick, J., R: Role of cations in CO₂ adsorption, dynamics, and hydration in smectite clays under in situ supercritical CO₂ conditions. *J. Phys. Chem. C.* **121**(1), 577–592 (2017). <https://doi.org/10.1021/acs.jpcc.6b11542>
- Busch, A., Alles, S., Gensterblum, Y., Prinz, D., Dewhurst, D.N., Raven, M.D., Stanjek, H., Krooss, B.M.: Carbon dioxide storage potential of shales. *Int. J. Greenh. Gas Control.* **2**(3), 297–308 (2008). <https://doi.org/10.1016/j.ijggc.2008.03.003>
- Busch, A., Amann, A., Bertier, P., Waschbusch, M., Krooss, B.M.: The significance of caprock sealing integrity for CO₂ storage. Society of Petroleum Engineers - SPE International Conference on CO₂ Capture, Storage, and Utilization 2010, 300–307. (2010)
- Busch, A., Bertier, P., Gensterblum, Y., Rother, G., Spiers, C.J., Zhang, M., Wentinck, H.M.: On sorption and swelling of CO₂ in clays. *Geomech. Geophys. Geo-Energy Geo-Resour.* **2**(2), 111–130 (2016). <https://doi.org/10.1007/s40948-016-0024-4>
- Creodoz, A., Bildstein, O., Jullien, M., Raynal, J., Trotignon, L., Pokrovsky, O.: Mixed-layer illite-smectite reactivity in acidified solutions: Implications for clayey caprock stability in CO₂ geological storage. *Appl. Clay Sci.* **53**(3), 402–408 (2011). <https://doi.org/10.1016/j.clay.2011.01.020>
- Du, X., Guang, W., Cheng, Y., Hou, Z., Liu, Z., Yin, H., Huo, L., Lei, R., Shu, C.: Thermodynamics analysis of the adsorption of CH₄ and CO₂ on montmorillonite. *Appl. Clay Sci.* **192** (2020). <https://doi.org/10.1016/j.clay.2020.105631>
- Dubinini, M.M., Astakhov, V.A.: Development of concepts of the volume filling of micropores in the adsorption of gases and vapors by microporous adsorbents - communication I. Carbon adsorbents. *Bull. Acad. Sci. USSR.* **20**(1), 17–22 (1971). <https://doi.org/10.1007/BF00849308>
- Dutta, P., Harpalani, S., Prusty, B.: Modeling of CO₂ sorption on coal. *Fuel.* **87**(10–11), 2023–2036 (2008). <https://doi.org/10.1016/j.fuel.2007.12.015>
- Fitzgerald, J.E., Sudibandriyo, M., Pan, Z., Robinson, R.L., Gasem, K.A.M.: Modeling the adsorption of pure gases on coals with the SLD model. *Carbon.* **41**(12), 2203–2216 (2003). [https://doi.org/10.1016/S0008-6223\(03\)00202-1](https://doi.org/10.1016/S0008-6223(03)00202-1)
- Fripiat, J.J., Cruz, M.I., Bohor, B.F., Thomas, J.: Interlamellar adsorption of carbon dioxide by smectites. *Clays Clay Min.* **22**(1), 23–30 (1974). <https://doi.org/10.1346/CCMN.1974.0220105>
- Galán, E., Aparicio, P.: Experimental study on the role of clays as sealing materials in the geological storage of carbon dioxide. *Appl. Clay Sci.* **87**, 22–27 (2014). <https://doi.org/10.1016/j.clay.2013.11.013>
- Giesting, P., Guggenheim, S., van Koster, A.F., Busch, A.: Interaction of carbon dioxide with Na-exchanged montmorillonite at pressures to 640bars: Implications for CO₂ sequestration. *Int. J. Greenh. Gas Control.* **8**, 73–81 (2012a). <https://doi.org/10.1016/j.ijggc.2012.01.011>
- Giesting, P., Guggenheim, S., Van Groos, K., A. F., and, Busch, A.: X-ray diffraction study of K- and Ca-exchanged montmorillonites in CO₂ atmospheres. *Environ. Sci. Technol.* **46**(10), 5623–5630 (2012b). <https://doi.org/10.1021/es3005865>
- Gil, A., Dachary, A.G., Korili, S.A.: Adsorption of CO₂ as a method for the characterisation of the structure of alumina-pillared clay catalysts. *Adsorption.* **15**(2), 203–210 (2009). <https://doi.org/10.1007/s10450-009-9168-7>
- Grekov, D.I., Suzuki-Muresan, T., Kalinichev, A.G., Pré, P., Grambow, B.: Thermodynamic data of adsorption reveal the entry of CH₄ and CO₂ in a smectite clay interlayer. *Phys. Chem. Chem. Phys.* **22**, 16727–16733 (2020)
- Horri, N., Sanz-Pérez, E.S., Arencibia, A., Sanz, R., Frini-Srasra, N., Srasra, E.: Effect of acid activation on the CO₂ adsorption capacity of montmorillonite. *Adsorption.* **26**(5), 793–811 (2020). <https://doi.org/10.1007/s10450-020-00200-z>
- Hunvik, K.W.B., Lima, R.J.S., Kirch, A., Loch, P., Røren, P.M., Petersen, M.H., Rudić, S., Sakai, V.G., Knudsen, K.D., Miranda, C.R., Breu, J., Fossum, J.O., Bordallo, H.N.: Influence of CO₂ on Nanoconfined Water in a clay Mineral. *J. Phys. Chem. C.* **126**(40), 17243–17254 (2022)
- Hur, T.B., Baltrus, J.P., Howard, B.H., Harbert, W.P., Romanov, V.N.: Carbonate formation in Wyoming montmorillonite under high pressure carbon dioxide. *Int. J. Greenh. Gas Control.* **13**, 149–155 (2013). <https://doi.org/10.1016/j.ijggc.2012.12.001>
- Hwang, J., Pini, R.: Enhanced sorption of supercritical CO₂ and CH₄ in the Hydrated Interlayer pores of Smectite. *Langmuir.* **37**(12), 3778–3788 (2021). <https://doi.org/10.1021/acs.langmuir.1c00375>
- Hwang, J., Joss, L., Pini, R.: Measuring and modelling supercritical adsorption of CO₂ and CH₄ on montmorillonite source clay. *Microporous Mesoporous Mater.* **273**, 107–121 (2019). <https://doi.org/10.1016/j.micromeso.2018.06.050>
- IPCC: In: Davidson, B.O., de Coninck, H.C., Loos, M., Meyer, L.A. (eds.) IPCC Special Report on Carbon Dioxide Capture and Storage. Prepared by Working Group III of the Intergovernmental Panel on Climate Change [Metz, p. 442. Cambridge University Press, Cambridge, United Kingdom and New York, NY, USA (2005)
- IPCC: An IPCC Special Report on the impacts of global warming of 1.5°C above pre-industrial levels and related global greenhouse gas emission pathways, in the context of strengthening the global response to the threat of climate change, sustainable development, and efforts to eradicate poverty [Masson-Delmotte. In: Zhai, V.P., Pörtner, H.-O., Roberts, D., Skea, J., Shukla, P.R., Pirani, A., Moufouma-Okia, W., Péan, C., Pidcock, R., Connors, S., Matthews, J.B.R., Chen, Y., Zhou, X., Gomis, M.I., Lonnoy, E., Maycock, T., Tignor, M., Waterfield, T. (eds.) Global Warming of 1.5°C, pp. 3–24. Cambridge University Press, Cambridge, UK and New York, NY, USA (2018). <https://doi.org/10.1017/9781009157940.001>
- Jedli, H., Jbara, A., Hedfi, H., Bouzgarrou, S., Slimi, K.: Carbon dioxide adsorption isotherm study on various cap rocks in a batch reactor for CO₂ sequestration processes. *Appl. Clay Sci.* **136**, 199–207 (2017). <https://doi.org/10.1016/j.clay.2016.11.022>
- Langmuir, I.: Adsorption of gases on plane surfaces glass, mica and platinum. *J. Am. Chem. Soc.* **40**, 1361–1403 (1918). <https://doi.org/10.1021/ja02242a004>

- 28 Li, M., Gu, A.Z.: Determination of the quasi-saturated vapor pressure of supercritical gases in the adsorption potential theory application. *J. Colloid Interface Sci.* **273**(2), 356–361 (2004). <https://doi.org/10.1016/j.jcis.2003.09.031>
- 29 Loganathan, N., Bowers, G.M., Yazaydin, A.O., Kalinichev, A.G., Kirkpatrick, R.J.: Competitive adsorption of H₂O and CO₂ in 2-Dimensional Nanoconfinement: GCMD simulations of Cs- and Ca-Hectorites. *J. Phys. Chem. C.* **122**(41), 23460–23469 (2018). <https://doi.org/10.1021/acs.jpcc.8b06602>
- 30 Loring, J.S., Ilton, E.S., Chen, J., Thompson, C.J., Martin, P.F., Bénézeth, P., Rosso, K.M., Felmy, A.R., Schaef, H.T.: In situ study of CO₂ and H₂O partitioning between Na-montmorillonite and variably wet supercritical carbon dioxide. *Langmuir.* **30**(21), 6120–6128 (2014). <https://doi.org/10.1021/la500682t>
- 31 Mahmoud, M., Hamza, A., Hussein, I.A., Eliebid, M., Kamal, M.S., Abouelresh, M., Shawabkeh, R., Al-Marri, M.J.: Carbon dioxide EGR and sequestration in mature and immature shale: Adsorption study. *J. Pet. Sci. Eng.* **188**, 106923 (2020). <https://doi.org/10.1016/j.petrol.2020.106923>
- 32 Mendel, N., Siretanu, D., Siretanu, I., Brilman, D.W.F., Mugele, F.: Interlayer Cation-Controlled Adsorption of Carbon Dioxide in Anhydrous Montmorillonite Clay. *J. Phys. Chem. C.* **125**(49), 27159–27169 (2021). <https://doi.org/10.1021/acs.jpcc.1c06746>
- 33 Merey, S., Sinayuc, C.: Analysis of carbon dioxide sequestration in shale gas reservoirs using experimental adsorption data and models. *J. Nat. Gas Sci. Eng.* **36**, 1087–1105 (2016). <https://doi.org/10.1016/j.jngse.2016.02.052>
- 34 Michels, L., Fossum, J.O., Rozynek, Z., Hemmen, H., Rustenberg, K., Sobas, P.A., Kalantzopoulos, G.N., Knudsen, K.D., Janek, M., Plivelic, T.S., Da Silva, G.J.: Intercalation and retention of carbon dioxide in a smectite clay promoted by interlayer cations. *Sci. Rep.* **5**, 2–10 (2015). <https://doi.org/10.1038/srep08775>
- 35 Molinard, A., Vansant, E.E.: Controlled Gas Adsorption properties of various Pillared Clays. *Adsorption.* **1**, 49–59 (1995)
- 36 Mudoi, M.P., Sharma, P., Khichi, A.S.: A review of gas adsorption on shale and the influencing factors of CH₄ and CO₂ adsorption. *J. Pet. Sci. Eng.* **217**, 110897 (2022)
- 37 Murata, K., Kaneko, K.: The general equation of supercritical gas adsorption isotherm. *J. Phys. Chem. B.* **105**(36), 8498–8503 (2001). <https://doi.org/10.1063/1.1344926>
- 38 Olabode, A., Radonjic, M.: Experimental investigations of caprock integrity in CO₂ sequestration. *Energy Procedia. Elsevier B V.* **37**, 5014–5025 (2013). <https://doi.org/10.1016/j.egypro.2013.06.415>
- 39 Ono, S., Kondo, S.: Molecular Theory of Surface Tension in liquids. *Struct. Liquids / Struktur Der Flüssigkeiten.* **255**(1858), 134–280 (1960). https://doi.org/10.1007/978-3-642-45947-4_2
- 40 Ottiger, S., Pini, R., Storti, G., Mazzotti, M.: Competitive adsorption equilibria of CO₂ and CH₄ on a dry coal. *Adsorption.* **14**(4–5), 539–556 (2008). <https://doi.org/10.1007/s10450-008-9114-0>
- 41 Pan, Z., Ye, J., Zhou, F., Tan, Y., Connell, L.D., Fan, J.: CO₂ storage in coal to enhance coalbed methane recovery: A review of field experiments in China. *Int. Geol. Rev.* **60**(5–6), 754–776 (2018). <https://doi.org/10.1080/00206814.2017.1373607>
- 42 Rao, S.N., Mathew, P.K.: Effects of exchangeable cations on hydraulic conductivity of marine clay. *Clays Clay Min.* **43**, 433–437 (1995). <https://doi.org/10.1346/CCMN.1995.0430406>
- 43 Raveendran, G., Arnepalli, D.N., Maji, V.B.: Effect of exchangeable cation on carbon dioxide adsorption in smectite clay. *Geo-Congress 2022: Geoenvironmental Engineering; Unsaturated Soils; Contemp. Top. Eros. Sustain. Coal Combust. Residuals.* 78–88 (2022). <https://doi.org/10.1061/9780784484050.009>
- 44 Reddy, M.S.B., Ponnamma, D., Sadasivuni, K.K., Kumar, B., Abdullah, A.M.: Carbon dioxide adsorption based on porous materials. *RSC Adv.* **11**, 12658–12681 (2021)
- 45 Rother, G., Ilton, E.S., Wallacher, D., Hau, T., Schaef, H.T., Qafoku, O., Rosso, K.M., Felmy, A.R., Krukowski, E.G., Stack, A.G., Grimm, N., Bodnar, R.J.: CO₂ sorption to subsingle hydration layer montmorillonite clay studied by excess sorption and neutron diffraction measurements. *Environ. Sci. Technol.* **47**(1), 205–211 (2012). <https://doi.org/10.1021/es301382y>
- 46 Schaef, H.T., Ilton, E.S., Qafoku, O., Martin, P.F., Felmy, A.R., Rosso, K.M.: In situ XRD study of Ca²⁺ saturated montmorillonite (STX-1) exposed to anhydrous and wet supercritical carbon dioxide. *Int. J. Greenh. Gas Control.* **6**, 220–229 (2012). <https://doi.org/10.1016/j.ijggc.2011.11.001>
- 47 Schaef, H.T., Loring, J.S., Glezakou, V.A., Miller, Q.R.S., Chen, J., Owen, A.T., Lee, M.S., Ilton, E.S., Felmy, A.R., McGrail, B.P., Thompson, C.J.: Competitive sorption of CO₂ and H₂O in 2:1 layer phyllosilicates. *Geochim. Cosmochim. Acta.* **161**, 248–257 (2015). <https://doi.org/10.1016/j.gca.2015.03.027>
- 48 Shannon, R.D.: Revised effective ionic Radii and systematic studies of interatomic distances in Halides and Chalcogenides. *Acta Crystallogr. A.* **32**, 751–767 (1976)
- 49 Span, R., Wagner, W.: A new equation of state for carbon dioxide covering the fluid region from the triple-point temperature to 1100 K at pressures up to 800 MPa. *J. Phys. Chem. Ref. Data.* **25**, 1509–1596 (1996). <https://doi.org/10.1063/1.555991>
- 50 Sudibandriyo, M., Mohammad, S.A., Robinson, R.L. Jr., Gasem, K.A.M.: Ono-Kondo lattice model for high-pressure adsorption: Pure gases. *Fluid. Phase. Equilibria.* **299**(2), 238–251 (2010). <https://doi.org/10.1016/j.fluid.2010.09.032>
- 51 War, K., Raveendran, G., Arnepalli, D.N.: Coupled hydromechanical model for evaluating the volume change and fluid permeation behavior of expansive clay smear in a fault upon interaction with CO₂. *Int. J. Greenh. Gas Control.* **119**, 103696 (2022). <https://doi.org/10.1016/j.ijggc.2022.103696>
- 52 Wu, K., Ye, Q., Wu, R., Chen, S., Dai, H.: Carbon dioxide adsorption behaviors of aluminum-pillared montmorillonite-supported alkaline earth metals. *J. Environ. Sci.* **98**, 109–117 (2020)
- 53 Yin, H., Zhou, J., Jiang, Y., Xian, X., Liu, Q.: Physical and structural changes in shale associated with supercritical CO₂ exposure. *Fuel.* **184**, 289–303 (2016). <https://doi.org/10.1016/j.fuel.2016.07.028>
- 54 Zhou, J., Liu, M., Xian, X., Jiang, Y., Liu, Q., Wang, X.: Measurements and modelling of CH₄ and CO₂ adsorption behaviors on shales: Implication for CO₂ enhanced shale gas recovery. *Fuel.* **251**, 293–306 (2019). <https://doi.org/10.1016/j.fuel.2019.04.041>

Publisher's Note Springer Nature remains neutral with regard to jurisdictional claims in published maps and institutional affiliations.

Springer Nature or its licensor (e.g. a society or other partner) holds exclusive rights to this article under a publishing agreement with the author(s) or other rightsholder(s); author self-archiving of the accepted manuscript version of this article is solely governed by the terms of such publishing agreement and applicable law.